656 *KSME International Journal, Vol. 13, No. 9, pp. 656~666, 1999*

Real Time Linear Simulation and Control for Small Aircraft Turbojet Engine

Chang Duk Kong* and Suk Choo Chung**

(Received April 20, 1998)

The performance of the aircraft gas turbine engine requires optimization because it is directly related to overall aircraft performance. In this study, a modified DYNGEN, a nolinear dynamic simulation program with component maps of the small aircraft turbojet engine, was used to predict the overall engine performance. Response characteristics of various cases, such as 6%, 5% and 3% rpm step models and the real-time linear model of the interpolation scheme within the operating range were compared. Among them, the real time linear model was selected for the turbojet engine with nonlinear characteristics. Finally control schemes such as PI (Proportional -Integral Controller) and LQR (Linear Quadratic Regulator) were applied to optimize the engine performance. The overshoot of the turbine inlet temperature was effectively eliminated by LQR controller with the proper control gain K.

Key Words: Turbojet Engine Performance, Nonlinear Dynamic Simulation, Real Time Linear Simulation and Control

Nomenclature

A, B, C	: System Matrix
a_{ij}, b_{il}, c_{kj}	: Element of Matrix
F	: Weighting Matrix of State Variable
f(•), g(•)	: Function of
G	: Weighting Matrix of Input Variable
J	: Performance Index
K	: Control Gain
K_i	: Integral Gain
K_p	: Proportional Gain
N	: Rotor Speed
P	: Pressure, [N/m^2]
S	: Matrix of Riccatti Equation
T	: Temperature, [K]
Δt	: Time Step, [sec]
u, x, y	: Vector
W_f	: Fuel Flow Rate

Subscripts

C	: Compressor
T	: Turbine
I, j, k, l	: Integer

Station Number of Figure

3	: Compressor Outlet
4	: Turbine Inlet
5	: Turbine Outlet

Acronyms

PI	: Proportion-Integral Controller
LQR	: Linear Quadratic Regular

* Dept. of Aerospace Engr., Chosun University
** Dept. of Mechanical Design Engr., Seoul National Polytechnic University

1. Introduction

For the requirements of optimal performance and high reliability in various operating ranges, dynamic simulation of the aero gas turbine engine is necessary to predict not only the engine performance but also the overall aircraft performance.

The simulation of aero engines with nonlinear characteristics has been derived for the actual engine performance modification or the engine design in the preliminary design phase. The dynamic simulation program which is available to predict the dynamic performance has continu-

ously developed (Fawke and Saravanamuttoo, 1971;Sellers and Daniele, 1975; Schoberi, et al., 1994).

Moreover, the application of the modern control scheme might be required. When the precise model is obtained, it is possible to design the optimal controller, which has been considered by several designers (Geyser, 1978; Bettocchi, et al., 1996).

Various types of controllers were designed for the purpose of system characteristics. They have been designed with the trial and error method in optimal conditions (Mahmoud and Mclean, 1991; Watts, et al., 1992).

In this study, nonlinear dynamic simulation program was developed from several change of the component maps of DYNGEN's block data which were based on the performance maps of a small aero engine. System matrices of the linear model were obtained for the DYGABCD code (Geyser, 1978).

These sample matrices were derived from the operating points in the scheduled range and then the least square method was applied to the interpolation between these sampling points, where each element of matrices was a function of the rotor speed.

Therefore, it could be available to simulate the linear model in real time. To prevent overshoot of the turbine inlet temperature, PI and LQR compensator were applied and compared.

2. Nolinear Dynamic Simulation

In this study, a small aircraft turbojet engine with a maximum diameter of 0.35m and a maximum length of 0.8m, a three-stage axial compressor, an annular type combustor, one-stage axial turbine, and a convergent nozzle without afterburner was used. (Fig. 1)

Recently, many dynamic simulation programs have been developed to simulate nonlinear engines (Stamatis, et al., 1990; Ismail and Bhinder, 1991).

The DYNGEN code has been utilized for nonlinear dynamic simulation (Seller and Daniele, 1975).

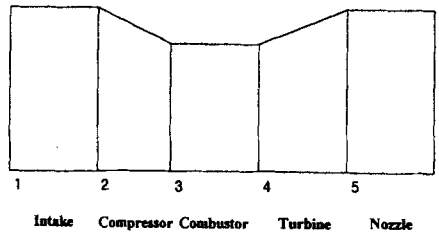

Fig. 1 Station No. of Single Shaft Turbojet Engine.

After modifying the block data of component maps in original code into new maps of a small aero gas turbine, which has been developed by an engine company in the Republic of Korea, nonlinear dynamic simulation was performed.

From the steady state simulation code for the engine, the necessary data were obtained in the format of block data of the DYGEN code. The corrected mass flow rate versus compressor efficiency and pressure ratio, the heating value versus combustor efficiency, and corrected rpm versus corrected turbine work function and turbine efficiency were derived. The component performance curves were constructed through the series calculation within each rpm.

The performance curve for the compressor was directly obtained from the steady state performance program in the format of DYGEN block data; that is, the corrected mass flow rate versus compressor efficiency and pressure ratio. However, combustor and turbine were not constructed because the resulting data from the steady state performance program did not fit the format of the DYNGEN block data.

Therefore, the steady state performance program in the range of 75% to 100% rpm and Mach No. 0 to 0. 9 was applied to calculate the steady values.

The following equation for the combustor efficiency was yielded with multiple regression (Wang, 1991;Ping and Saravanamuttoo, 1992).

$$\eta_b = a + b \cdot \Delta T + c \cdot P_3 + d \cdot \Delta T \cdot P_3 + e \cdot (\Delta T)^2 - f \cdot (P_3)^2 \quad (1)$$

where, a, b, c, d, e, and f are coefficients of multiple regression (Table 1). The pressure drop between the inlet and outlet of the combustor is neglected. Even though the combustor pressure

Table 1 Coefficients of multiple regression for obtaining performance curve.

Coeffi'	ETAB	DHTC	ETAT
a	0.976304	0.42167	0.000512
b	1.883E-6	0.11391	2.42618
c	7.1449E-6	-0.01440	-0.4576
d	1.0707E-9	0.03553	-0.0471
e	-4.1399E-9	-0.01950	·
f	-9.3803E-10	-0.2110	·

Table 2 Design point of a small single shaft turbojet engine.

	Design Point (Case 1)	Design Point (Case 2)
Altitude	0 Km	1.527 Km
Mach No.	0	0.6
Fuel Flow Rate	0.0441 Kg/s	0.0663 Kg/s
Comp' PR	3.5	3.47
Comp' Effi'	0.7914	0.7894
Air Flow Rate	5.814 Kg/s	6.173 Kg/s
Combustor Effi'	0.99	0.99
TIT	1065.3 K	1048 K
Turbine Effi'	0.8354	0.83
RPM	27999	28049

loss was considered in performance simulation, it could be neglected for simplicity to express the combustor efficiency equation through multiple regression.

From Eq. (1), the performance curve of the combustor was obtained, which could be used in DYNGEN for 1500, 2000, 2500, 3000, 4000, and 5000 mbar of combustor pressure with a change in the combustor temperature from 169 to 852K.

Also using a similar method, the performance curve of the turbine was constructed.

The following equations were then used to obtain the turbine work function (DHTC) and turbine efficiency (ETAT).

$$DHTC=a+b\cdot N+c\cdot T+d\cdot N\cdot T+e\cdot N\sqrt{T}+f\cdot\sqrt{N}\sqrt{T}, \quad (2)$$

$$ETAT=a+b\cdot N+c\cdot N\sqrt{T}+d\cdot N^2\sqrt{T}, \quad (3)$$

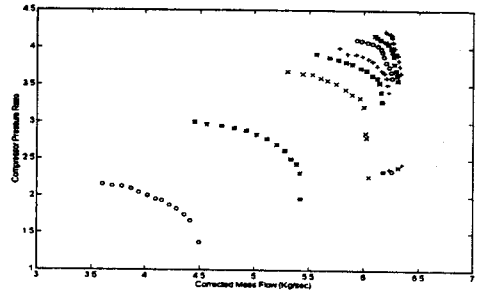

Fig. 2 Performance Curve of Compressor.

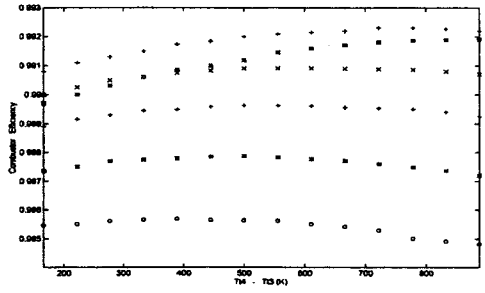

Fig. 3 Performance Curve of Combustor.

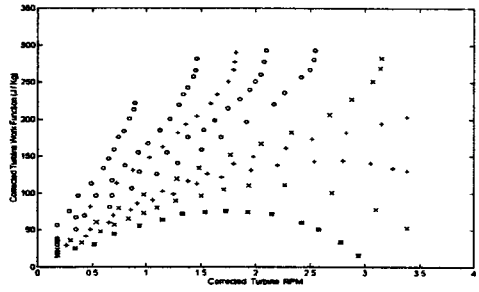

Fig. 4 Performance Curve of Turbine.

where each coefficient of each equation was shown in Table 1.

However, the turbine operating range was narrow; the turbine flow function (TFF) was between 12. 6 and 13. 6, the corrected rpm (CN) was between 1. 80 and 2.28, and the corrected work function (DHTC) was between 0.022 and 0. 037.

Considering the similarity of an axial turbine, the high pressure turbine of the original DYNGEN code could be used for this turbine (Stamatis, et al., 1990).

Using the following equations, the scaling factor was calculated in the range of 3.4 to 3.7

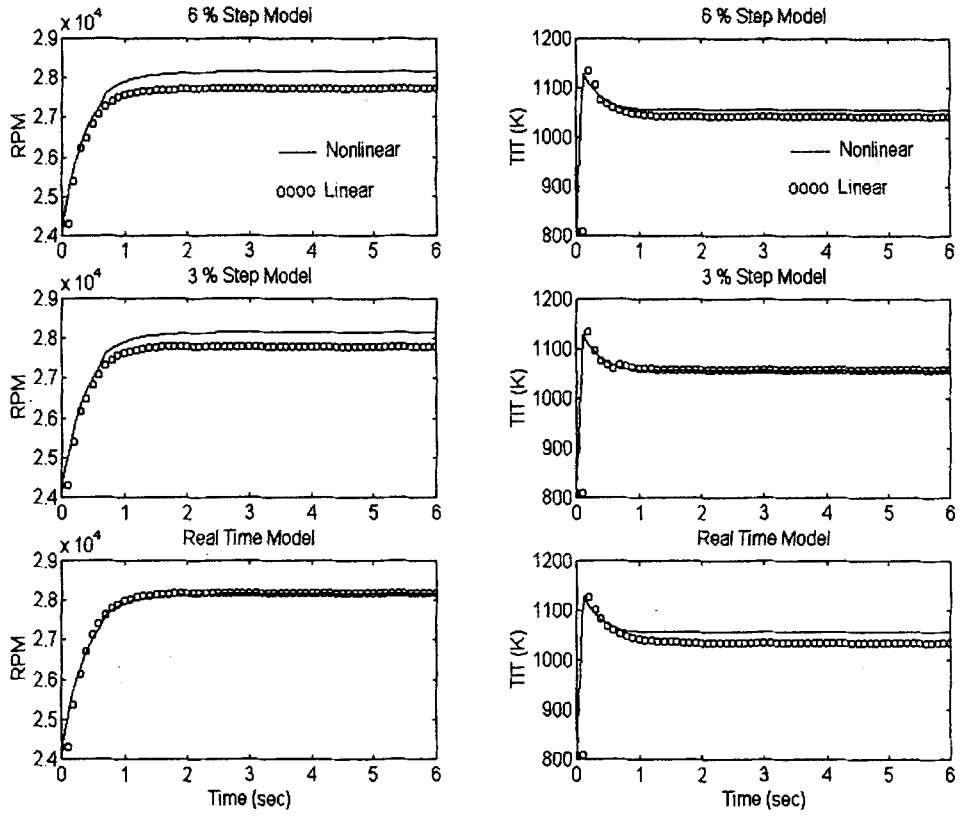

Fig. 5 Response of Various Linear Models in RPM and TIT Case 1 with 79% rpm to 94% rpm.

$$WA=\frac{(WA)_{design}}{(WA)_{map,design}}\times(WA)_{map}, \quad (4)$$

$$PR=\frac{(PR)_{design}-1}{(PR)_{map,design}-1}\times[(PR)_{map}-1]+1, \quad (5)$$

$$ETA=\frac{(ETA)_{design}}{(ETA)_{map,design}}\times(ETA)_{map}, \quad (6)$$

where, PR is the pressure ratio, WA is the mass flow rate, and ETA is the isothermal efficiency of the turbine, respectively.

In order to fit the small turbojet engine, the value of TFF was reduced by 3.5 times from the original TFF value of DYNGEN. However, the original characteristics were not changed, and the compressor map and the combustor map were derived from the small turbojet engine. (Fig. 2, 3, 4)

In the above process, the modified DYNGEN was obtained, and the nonlinear simulation results were compared with the various linear simulations in Fig. 5, Table 5, 6, 7 and 8.

3. Linear Model of Nonlinear Engine and Real Time Simulation

3.1 Linear model of nonlinear engine

To apply the modern control scheme, linearization of the nonlinear engine might be required.

A nonlinear time invariant system is expressed as follows:

$$\text{State equation}: \dot{x}=f(x, u), \quad (7)$$

$$\text{Output equation}: y=g(x, u), \quad (8)$$

where, x, $x\in R_n$, $y\in R_m$, and $u\in R_r$, respectively.

Expanding Eqs. (7), and (8) about an arbitrary operating point(x_s, u_s) with the Taylor expansion series, and neglecting higher order terms, the nonlinear system can be expressed by the following linearized state equation,

$$\begin{aligned}\delta\dot{x}&=A\delta x+B\delta u,\\ \delta y&=C\delta x,\end{aligned} \quad (9)$$

where, $\delta x=x-x_s$, $\delta \dot{x}=\dot{x}-\dot{x}_s$, $\delta y=y-y_s$, $\delta u=u-u_s$, $y_s=g(x_s, u_s)$, and $\dot{x}_s=f(x_s, u_s)$, respectively.

The state matrix A, the control matrix B, and the output matrix C are $n\times n$, $n\times r$, and $m\times n$ matrix, respectively.

$$A=[a_{ij}]=[\partial f_i/\partial x_j], \quad (10)$$
$$B=[b_{il}]=[\partial f_i/\partial u_l], \quad (11)$$
$$C=[c_{kj}]=[\partial g_k/\partial x_j], \quad (12)$$

where, $I=1, 2, \cdots, n$, $j=1, 2, \cdots, n$, $k=1, 2, \cdots, m$, and $l=1, 2, \cdots, r$.

Using DYGABCD, the A, B matrices were obtained for the partial difference of 2% about operating points, and the output matrix C was fixed as C=[1 0 0].

The state space equation has state variables such as rotor speed, compressor outlet pressure, turbine inlet temperature. The fuel flow rate is control input, and the rotor speed is an output variable.

Therefore

$$\begin{aligned}\delta x&=[\delta N \ \delta P_3 \ \delta T_4 \ \delta T_5]^T\\ \delta u&=\delta \dot{W}_f\\ \delta y&=\delta N\end{aligned} \quad (13)$$

3.2 Real time linear simulation and numerical solutions

Since the state variable changes with rotor speed, matrices of state space equations must be changed as the rotor speed changes (Kerr, et al., 1992; Mihaloew, et al., 1984; Smith and Stammetti, 1990a). In real time linear simulation, first of all, scheduled sampling data were needed. To minimize errors and the time of calculation, proper sampling data are needed. Various linear models, which are the 6%, 5%, 3% rpm step models, and the real time piecewise linear model with various environmental conditions such as Mach No. of 0 and an altitude of 0 km and Mach No. of 0.6 and an altitude of 1,570 km, were considered.

The least square method for the real time piecewise linear model was shown to be as follows.

First of all, in operating points $x_i (i=0, 1, 2, ..., n)$, if the approximate function $p(x)$ and the original function $f(x)$ are in the following relation,

$$f_i=f(x_i)-P(x_i), \ (i=0, 1, 2, \cdots, n) \quad (14)$$

the least square method is applied. Then,

$$\sum_{i=0}^{n} f_i^2=\sum_{i=0}^{n}[f(x_i)-p(x_i)]^2 \quad (15)$$

where, the approximate function $p(x)$ is the n th order polynomial,

$$p(x)=a_0+a_1x+a_2x^2+\cdots+a_nx^n \quad (16)$$

The sampling data of the state matrix A and the control matrix B are functions of the engine rotor speed, and their coefficients are shown in Tables 3 and 4.

Table 3 Coefficients of polynomials for elements of matrix A, B for case 1.

	Elements of matrix A, B				
Coeffi'	A(1, 1)	A(2, 2)	A(3, 3)	A(4, 4)	B(1, 1)
a_3	0.00	0.00	-0.0001	0.00	-0.4
a_2	-0.0019	-0.2	0.0133	0.2	51.9
a_1	0.117	11.8	-1.1616	-12	-1491.1
a_0	-11.335	-1253.3	-375.16	-4321.4	-4009.8

Table 4 Coefficients of polynomials for elements of matrix A, B for case 2.

	Elements of matrix A, B				
Coeffi'	A(1, 1)	A(2, 2)	A(3, 3)	A(4, 4)	B(1, 1)
a_3	-0.001	0.2	-0.008	-0.2	-11.4
a_2	0.0131	-5	0.2179	5.4	492.5
a_1	0.0315	41	-3.345	-75.5	-5251
a_0	-13.61	-1382	-370.8	-4222	345.1

3.3 The comparisons of nonlinear and various linear simulation

In the nonlinear and the linear simulation for the small gas turbine engine, the fuel flow rate as an input was considered. The rpm response and turbine inlet temperature response were compared.

In case 1, the fuel flow rate was 0.0441 kg/s

step input, it was applied from 79% rpm to 94% rpm. (Fig. 5) As shown in Table 5, in the rpm response, the settling time for the 3% rpm step model was 0.4 seconds faster than that of the nonlinear model. But the steady state error of the real-time was 0.04% so that the real-time model was close to the nonlinear model.

Also in the turbine inlet temperature (TIT),

Table 5 Comparison of various simulation results based on RPM in step input for case 1.

	Nonli'	6% Step	3% Step	Real Time
Settling Time	3.0	3.08	2.6	3.04
S-State Value (Err%)	28157	27711	27794	28169
	(0)	(1.58)	(1.29)	(0.04)
Over-shoot	0	0	0	0

Table 6 Comparison of various simulation results based on TIT in step input for case 1.

	Nonli'	6% Step	3% Step	Real Time
Settling Time	2.8	1.88	1.52	3.44
S-State Value (Err%)	1055.8 K	1039.4 K	1055.2 K	1034.1 K
	(0)	(1.56)	(0.06)	(2.06)
Over-shoot	1127.7 K	1154.4 K	1155.4 K	1144.9 K
	6.8%	11.2%	9.5%	10.7%

Table 7 Comparison of various simulation results based on RPM in step input for case 2.

	Nonli'	5% Step	3% Step	Real Time
Settling Time	2.1	2.0	2.2	2.2
S-State Value (Err%)	28394.4	27505	28172	28406
	(0)	(3.13)	(0.78)	(0.04)
Over-shoot	0	0	0	0

Table 8 Comparison of various simulation results based on TIT in step input for case 2.

	Nonli'	5% Step	3% Step	Real Time
Settling Time	19	23	18	1.8
S-State Value (Err%)	1052.8 K	1075.3 K	104.8 K	1055.1 K
	(0)	(2.14)	(0.4)	(0.22)
Over-shoot	1141.2 K	1140 K	1140 K	1128 K
	8.4%	6.02%	8.8%	6.91%

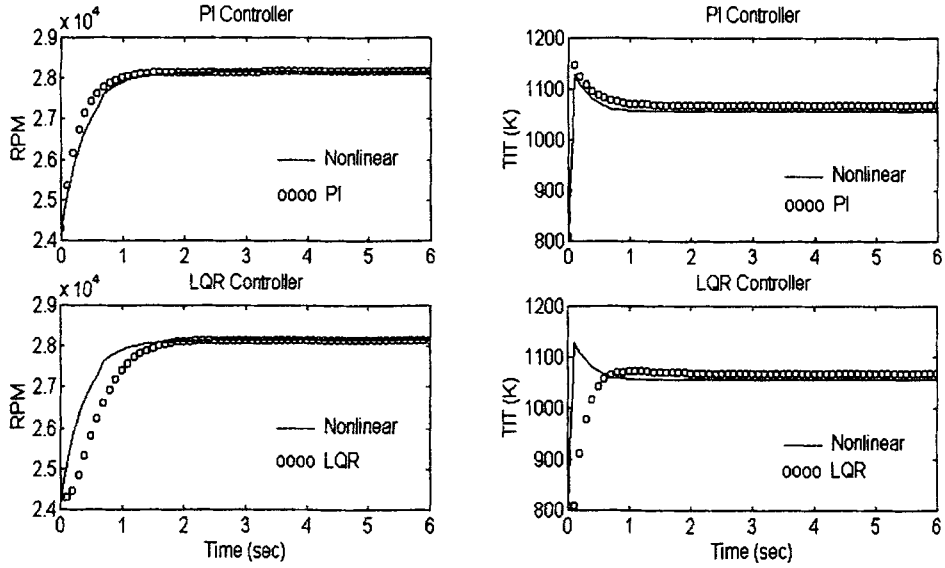

Fig. 6 Response of PI and LQR Controller in RPM and TIT for Case 1 with 79% rpm to 94 rpm.

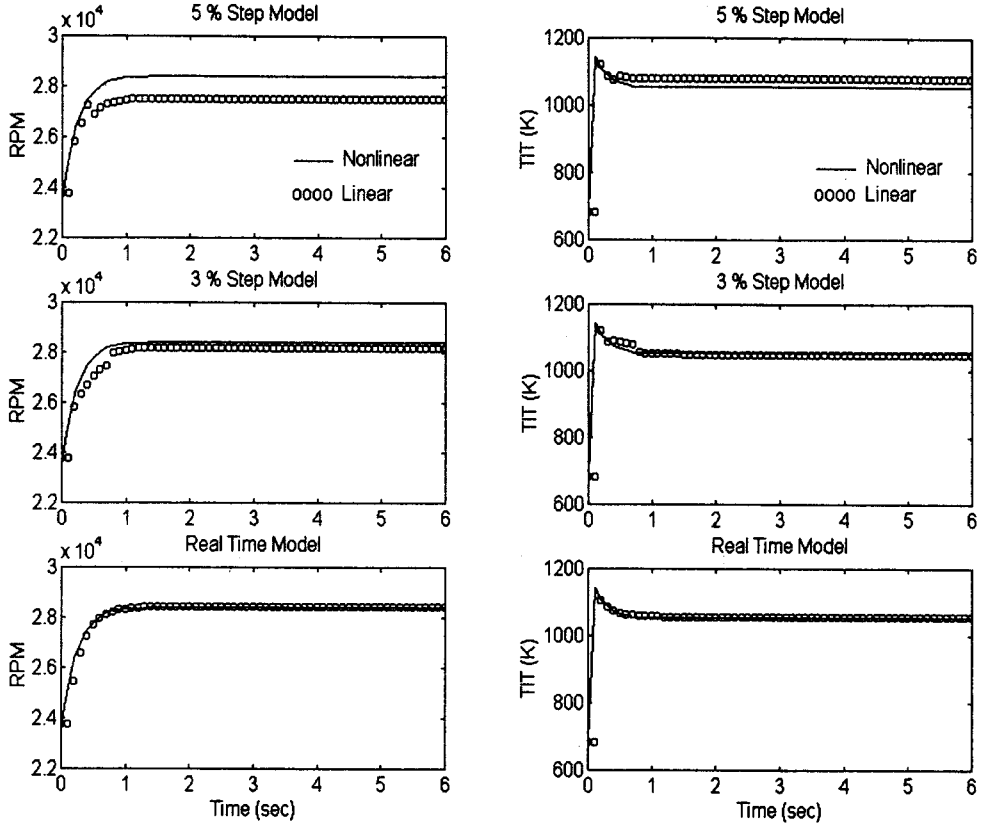

Fig. 7 Response of Various Linears Models in RPM and TIT for Case 2 with 80% rpm to 95% rpm.

the real-time model was twice as fast as that of the nonlinear model in tyhe settling time. But the 3% rpm step model was only 0.06% in steady state error. (Table 6)

In case 2, the fuel flow rate was 0. 0663 kg/s step input, it was applied from 80% rpm to 95% rpm. (Fig. 7)

As shown in Table 7, in rpm response, the settling time for the 5% rpm step model was 0. 1 second faster than that of the nonlinear model. But the steady state error of the real-time model was 0.04%

For TIT as shown in Table 8, in settling time, the 3% rpm step model and the real-time model were 0.1 second faster than the nonlinear model, and the real-time model had a 0.22% steady state error.

In the overshoot of TIT, the nonlinear model had an overshoot of 88.4K and the 5% rpm step model had an overshoot of 64.7K

Therefore, as mentioned above, it was recognized why TIT has a limitation. The overshoot causes engine failure because of serious turbine thermal stress.

4. Design of the Controller

As shown in the above results, the real-time piecewise linear model had satisfactory response characteristics, which were very close to the nonlinear model, but it still had an overshoot of the turbine inlet temperature.

Since the overshoot of the turbine inlet temperature affects failure due to turbine thermal stress, it should be minimized with proper response time.

The real-time linear model must be considered to design a controller with controllability and stability.

Therefore, controllable matrix Mc is assumed as follows,

$$Mc=[B : AB : A^2B : \cdots : A^{n-1}B], \quad (17)$$

where matrix A is $n\times n$ and matrix B is $n\times r$, respectively.

If the rank of controllable matrix is equal to n, this model is controllable, But if it is less than n, this model is not controllable.

The real time linear model in this study was controllable and stable.

To eliminate the turbine inlet temperature overshoot effectively, the classical PI controller and the modern optimal LQR controller were designed, and their results were compared (Kong and Han, 1995; Smith and Stammetti, 1990b).

4.1 Design of The classical PI controller

The classical PI controller has been widely used because of its robustness (Math Work, Inc. 1992). Proportional elements tend to reduce the steady state error with an increase of the proportional gain, and integral elements have damping effects on the overshoot of system responses. The PI controller is shown as follows,

$$m(t)=K_p(\Delta(t)+K_I\int_0^t \Delta(\lambda)\,d\lambda), \quad (18)$$

where Δ is control input, $m(t)$ is control output, and λ is the dummy variable of integration, respectively.

Therefore, the transfer function of PI controller is shown as follows,

$$G_c(s)=\frac{M(s)}{\Delta(s)}=K_p\left[1+\frac{K_I}{s}\right]=K_p\left[\frac{s+K_I}{s}\right] \quad (19)$$

By using the characteristics of each elements of PI controller, the value of each gain, which was compared with many different values, was chosen to control effectively the overshoot of the turbine inlet temperature.

Integral gains and proportional gains for each case are as follows,

$$\begin{aligned} &K_i=0.001,\ K_p=0.27 \text{ for case 1}\\ &K_i=0.001,\ K_p=0.54 \text{ for case 2} \end{aligned} \quad (20)$$

4.2 Design of the modern optimal LQR controller

The optimal linear quadratic regular (LQR), which has been widely used as a modern control scheme, was developed by Kalman in 1960 (Merrill, et al., 1984;Garg, 1996).

The plant state equation of the LQR controller is shown as,

$$\dot{x}=Ax+Bu, \quad (21)$$

where the initial state x(0) is given, and $x\in R^n$, $u\in R^m$, respectively.

The cost function J to determine the optimal control u(0) is defined as follows,

$$J=\int_0^\infty (\delta x^T F\delta x+\delta u^T G\delta u)\,dt, \quad (22)$$

where F is a real symmetric $n\times n$ positive semidefinite matrix. and G is a real symmetric $m\times m$ positive definite matrix.

If the optimal control is unique and all states are observable, the optimal control law yields as follows,

$$\delta u=K\delta x=-G^{-1}B^TS\delta x, \quad (23)$$

where S is the positive semidefinite matrix and the unique solution for the following equation is

$$0=SA+A^TS+F-SBG^{-1}G^TS \quad (24)$$

Therefore, in order to design a LQR controller, the selection of F and G are needed and there are there are various methods, the one employed for this study is shown as follows,

in case 1,

$$F=[19200]$$
$$G=\left[\frac{1}{19200}\right]I,$$

and in case 2,

$$F=[18500]$$
$$G=\left[\frac{1}{18500}\right]I,$$

where I is the identity matrix.

The control gain K was obtained by MATLAB (Math Works, Inc., 1992) as follows

in case 1,

$$K(t)=[0.0308\ 0.6469\ 0.0108-0.0002]\times 10E-03, \quad (27)$$

and in case 2,

$$K(t)=[0.0307\ 0.6554\ 0.0141-0.0004]\times 10E-02 \quad (28)$$

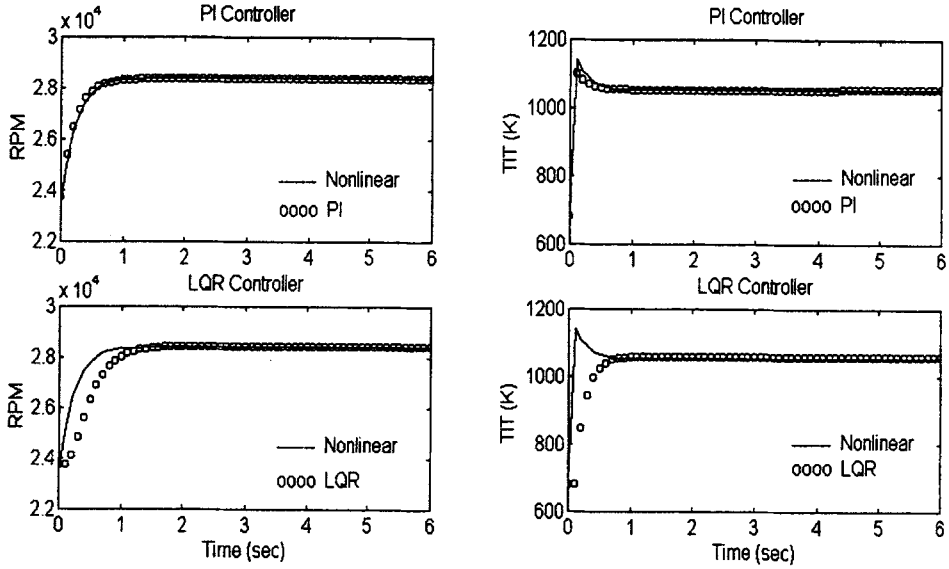

Fig. 8 Response of PI and LQR Controllers in RPM and TIT for Case 2 with 80% rpm to 95% rpm.

Table 9 Comparison of control results with PI and LQR controller in step input for case 1.

	RPM			TIT		
	NonLi	PI	LQR	NonLi	PI	LQR
Settl' time	3.0	2.5	3.3	2.8	5.4	5.1
S-S value (Err%)	28157	28147	28150	1055.8	1067.7	1067.1
	(0)	(0.03)	(0.02)	(0)	(1.13)	(1.06)
Over-shoot	0	0	0	1127.7	1145.1	1071.4
				6.8%	7.25%	0.41%

Table 10 Comparison of control results with PI and LQR controller in step input for case 2.

	RPM			TIT		
	NonLi	PI	LQR	NonLi	PI	LQR
Settl' time	2.1	1.7	2.7	1.8	1.4	2.0
S-S value (Err%)	28394	28352	28417	1052.8	1051	1056.3
	(0)	(0.15)	(0.08)	(0)	(0.17)	(0.33)
Over-shoot	0	0	0	1141.2	1130	1052.8
				8.4%	7.51%	0%

4.3 Comparison of control results

As mentioned above, for the step input, all of the nonlinear and real-time linear models had an overshoot of TIT. Therefore, the PI and LQR controllers were designed to eliminate the overshoot of TIT.

In Table 9, for 0. 0441kg/s step input (Fig. 6), the rpm response of PI controller was 0. 8 seconds faster than that of LQR controller, and the steady state errors of each of the controllers were 0.03% and 0.02%, respectively.

In attempting to control the overshoot of TIT, the setting time of each controller was 5. 4 seconds, which was twice that of the nonlinear model. The steady state errors of each controller were over 1%.

The overshoot of TIT was effectively eliminated by LQR controller, but not by PI controller. (Table 9)

In Table 10, for 0.0663kg/s step input (Fig. 8), the settling time of PI controller was 0.6 seconds faster than that of LQR controller, which had a 0. 08% rpm response steady state error. In this case, the overshoot of PI controller was 7.51%, but LQR controller eliminated it effectively.

5. Conclusions

For nonlinear simulations, the DYNGEN program, which can easily be modified by users, was employed. To obtain the performance curves in the format of DYGEN block data, modified maps were constructed with the performance data from the steady state performance program by using the multiple regression. The modified DYNGEN was obtained, and the simulation results conformed closely with the experimental characteristics of the small gas turbine engine.

For linear simulation, various linear models such as the 6%rpm step, the 5% rpm step, the 3% rpm step and the real-time linear model were considered. In two different environmental conditions, the real-time linear characteristics in rpm and turbine inlet temperature were obtained.

To eliminate the overshoot of the turbine inlet temperature, after observing controllability and stability of the real-time linear model, two controllers, PI and LQR controller, were designed. In comparison, LQR controller was more effective in eliminating the overshoot of TIT than PI controller.

References

(1) Bettocchi, R., Spina P. R., and Fabbri, F., 1996, "Dynamic Modeling of Single-Shaft Industrial Gas turbine," *ASME 96-GT-332.*

(2) Fawke A. J., Saravanamuttoo, H.I. H., 1971, "Experimental Investigation of Methods for Improving the Dynamic Response of a Twin -Spool Turbojet Engine," *J. of Eng. for Power*, pp. 418~424.

(3) Garg, S. , 1996, "A simplified Scheme for Scheduling Multivariable Controllers and Its Application to a Turbofan Engine," *ASME 96 -GT-104.*

(4) Geyser, L. C., 1978, "*DYGABCD-a Program for Calculating Linear A, B, C, D Matrices from a Nonlinear Dynamic Engine Simulation*," NASA TP 1295.

(5) Kerr, L. J., Nemec, T. S., and Gallops, G. W., 1992, "Real Time Estimation of Gas Turbine Damage Using a Control-Based Kalman Filter Algorithm," *J. of Eng. for Gas Turbines and Power*, vol. 114, pp. 187~195.

(6) Kong, C. D., Han, M. S., 1995, "A Turbojet Engine LQR Control Using Linear Simulator," *J. of KSAS*, Vol. 23, pp. 9~15.

(7) Ismail, I. H., Bhinder, F. S., 1991, "Simulation of Aircraft Gas Turbine Engines," *J. of Eng. for Gas Turbines and Power*, Vol. 113, pp. 95~99.

(8) Mahmoud, S., and McLean, D., 1991, "Effective Optimal Control of an Aircraft Engine," Aeronautical Journal, pp. 21~27.

(9) Math Works Inc., 1992, "*Control System Toolbox User's Guide*," Natrick, Massachusetts, U. S. A.

(10) Merrill, W., Lehtinen, B., and Zeller, J., 1984, "The Role of Modern Control Theory in the Design of Control for Aircraft Turbine Engines," *J. of Guidance*, Vol. 7, No. 6, pp. 652~661.

(11) Mihaloew, J. R., Roth, S. P., and Creekmore, R., 1984, "Real Time Pegasus Propulsion System Model V/STOL-Piloted Simulation Evaluation," *J. of Guidance*, Vol. 7, No. 1, pp. 77~84.

(12) Ping, Z., Saravanamuttoo, H. I. H., 1992, "Simulation of an Advanced Twin-Spool Industrial Gas Turbine," *J. of Gas Turbines and Power*, Vol. 114, pp. 180~186.

(13) Schobeiri, M. T., Attia, M., Lippke, C., 1994, "GETRAN: A Greneric, Modularly Structured Computer Code for Simulation of Dynamic Behavior of Aero and Power Generation Gas Turbine Engines," *J. of Gas Turbines and Power*, Vol. 116, pp. 483~494.

(14) Sellers, J. F., and Daniele, C. J., 1975 "DYGEN - *A Program for Calculating Steady-State and Transient Performance of Turbojet and Turbofan Engines*," NASA TN D-7901.

(15) Smith, D, L., and Stammetti, V. A., 1990a, "Sequential Linearization as an Approach to Real-Time Marine Gas Turbine Simulation," *J. of Eng. for Gas Turbines and Power*, Vol. 112, pp. 187~191.

(16) Smith, D. L., and Stammetti, V. A., 1990b,

"Comparative Controller Design for a Marine Gas Turbine Propulsion System," *J. of Eng. for Gas Turbines and Power*, Vol. 112, pp. 182~186.

(17) Stamatis, A., Mathioudakis, K, Papailiou, K. D., 1990, "Adaptive Simulation of Gas Turbine Performance," *J. of Eng. for Gas Turbines and Power*, Vol. 112, pp. 168~175.

(18) Sugiyama, N., 1994, "Derivation of System Matrices from Nonlinear Dynamic Simulation of Jet Engines," *J. of Guidance*, Vol. 17, NO. 6, pp. 1320~1326.

(19) Wang, Y., 1991, "A New Method of Predicting the Performance of Gas Turbine Engines," *J. of Eng. for Gas Turbines and Power*, Vol. 113, pp. 106~111.

(20) Watts, J. W., Dwan, T. E., and Brockus, C. G., 1992, "Optimal State-Space Control of a Gas Turbine Engine," *J. of Eng. for Gas Turbines and Power*, Vol. 114, pp. 763~767.

(21) Kong, C. D. and Kim, S. K., 1997, "Real Time Linear Simulation and Control for The Small Aircraft Turbojet Engine," *ASME '97 Congress & Exhibition, Paper* No. 97-AA-114.